

# Calculation of Three-Dimensional Boundary Layers

## I. Swept Infinite Cylinders and Small Cross Flow

TUNCER CEBECI\*

*Douglas Aircraft Company, Long Beach, Calif.*

This paper presents a general method for solving the laminar and turbulent boundary-layer equations for swept infinite cylinders and for small cross flows. In the equations the Reynolds shear stress terms are eliminated by using an eddy viscosity concept. A very efficient and accurate two-point finite-difference method used earlier by Keller and Cebeci for two-dimensional flows is used to solve the governing equations. The accuracy of the method is investigated for several flows by comparing the calculated results with experiment and with those obtained by Bradshaw. In general, the agreement with experiment and with Bradshaw's results are quite satisfactory.

### Nomenclature

$A$	= Van Driest damping parameter
$b$	= $1 + \varepsilon^+$
$c_{f_s}, c_{f_x}, c_{f_z}$	= local skin-friction coefficients in the streamwise, chordwise and spanwise directions, respectively
$f$	= dimensionless stream function
$g$	= $\int_0^\eta (w/w_e) d\eta$
$h_1, h_2$	= metric coefficients, wherever applicable
$K$	= variable grid parameter
$K_1, K_2$	= geodesic curvatures
$L$	= modified mixing length
$p^+$	= dimensionless pressure gradient parameter
$R_s, R_x$	= Reynolds number, $u_s s/\nu$ and $u_e x/\nu$ , respectively
$R_{\delta_1}^*, R_{\theta_{11}}$	= Reynolds number $u_s \delta_1^*/\nu$ and $u_s \theta_{11}/\nu$ , respectively
$s$	= distance along inviscid streamline on surface of body
$u, v, w$	= velocity components in the $x, y, z$ directions or in the $s, y, z$ directions, respectively
$u_\tau$	= friction velocity
$y$	= distance normal to the body surface
$z$	= distance normal to the $x$ -coordinate or $s$ -coordinate, wherever applicable
$\alpha$	= parameter in the outer eddy viscosity formula
$\beta$	= cross-flow angle
$\delta$	= boundary-layer thickness
$\delta_1^*$	= displacement thickness, $\int_0^\infty (1 - u_s/U_s) dy$
$\varepsilon_1$	= eddy viscosity
$\varepsilon^+$	= dimensionless eddy viscosity, $\varepsilon_1/\nu$
$\eta$	= similarity variable
$\theta_{11}$	= momentum thickness, $\int_0^\infty \frac{u_s}{U_s} \left(1 - \frac{u_s}{U_s}\right) dy$
$\lambda$	= sweep angle
$\mu$	= dynamic viscosity
$\nu$	= kinematic viscosity
$\rho$	= density
$\tau$	= shear stress
$\psi$	= stream function
$\phi$	= local freestream angle

### Subscripts

$e$	= boundary-layer edge
$s$	= streamwise direction
$w$	= wall
$x$	= chordwise direction
$z$	= spanwise direction
$\infty$	= reference conditions

### Superscript

' = denotes differentiation with respect to  $\eta$

## 1. Introduction

IN this paper we present a general method for solving the laminar and turbulent boundary-layer equations for swept infinite cylinders and for small cross flows. The method utilizes the eddy viscosity concept to model the Reynolds shear stress terms and employs a very efficient and accurate two-point finite-difference method used earlier by Keller and Cebeci for two-dimensional boundary layers.<sup>1,2</sup> The expressions used for the eddy viscosity formulas are an extension of the expressions used by Cebeci<sup>3,4</sup> for two-dimensional flows.

The method is tested for accuracy and for computation speed for a number of turbulent flows past infinite swept wings and plates. The computed results are compared with the available experimental data and with Bradshaw's method.<sup>5</sup> For most cases the results indicate good agreement with experiment and agree fairly well with Bradshaw's calculated results. The results also indicate that the computation time of the method is quite small. A typical infinite swept wing can be calculated in approximately  $\frac{1}{2}$  min on the IBM 370/165.

## 2. The Boundary-Layer Equations

The governing boundary-layer equations for three-dimensional incompressible flows in streamline coordinates are given by the following equations:

Continuity

$$(\partial/\partial x)(h_2 u) + (\partial/\partial z)(h_1 w) + (\partial/\partial y)(h_1 h_2 v) = 0 \quad (1)$$

Streamwise Momentum

$$\begin{aligned} \frac{u}{h_1} \frac{\partial u}{\partial x} + \frac{w}{h_2} \frac{\partial u}{\partial z} + v \frac{\partial u}{\partial y} - uwK_2 + K_1 w^2 = \\ - \frac{1}{\rho h_1} \frac{\partial p}{\partial x} + \frac{1}{\rho} \frac{\partial}{\partial y} \left( \mu \frac{\partial u}{\partial y} - \rho \overline{u'v'} \right) \end{aligned} \quad (2)$$

Cross-Flow Momentum

$$\begin{aligned} \frac{u}{h_1} \frac{\partial w}{\partial x} + \frac{w}{h_2} \frac{\partial w}{\partial z} + v \frac{\partial w}{\partial y} - K_1 uw + K_2 u^2 = \\ - \frac{1}{\rho h_2} \frac{\partial p}{\partial z} + \frac{1}{\rho} \frac{\partial}{\partial y} \left( \mu \frac{\partial w}{\partial y} - \rho \overline{w'v'} \right) \end{aligned} \quad (3)$$

The preceding coordinate system is an orthogonal coordinate system formed by the inviscid streamlines and their orthogonal trajectories on the surface. As seen in Fig. 1, the projection of the freestream velocity vector on the surface is aligned with the

Received July 25, 1973; revision received December 26, 1973. This work was supported by the Naval Ship Research and Development Center under Contract N00014-72-C-0111, Subproject SR 009 01-01.

Index category: Boundary Layers and Convective Heat Transfer—Turbulent.

\* Manager, Viscous Flows Research. Member AIAA.

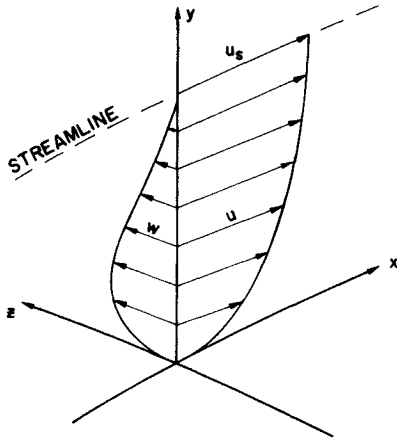


Fig. 1 Streamline coordinate system.

surface coordinate  $x$ . The velocity component along the  $z$ -axis, referred to as the cross-flow velocity, is zero at the edge of the boundary layer. For a three-dimensional flow the velocity vector at any  $y$ -location in the boundary-layer differs in direction from the freestream vector when both are projected on the surface. In that case the cross-flow velocity  $w$  within the boundary layer differs from zero (except at the wall). The departure of the velocity vector within the boundary layer is conveniently represented by the cross-flow angle  $\beta$  defined as  $\beta = \tan^{-1}(w/u)$ . That formula is indeterminate at  $y = 0$ ; however, with the use of L'Hospital's Rule, it can be written as  $\beta = \tan^{-1}(\partial w/\partial y)_w(\partial u/\partial y)_w^{-1}$ .

In Eqs. (1–3),  $h_1$  and  $h_2$  are metric coefficients, which are functions of  $x$  and  $z$ . The parameters  $K_1$  and  $K_2$  are known as the geodesic curvatures of the curves  $x = \text{const}$  and  $z = \text{const}$ , respectively. They are defined by

$$K_1 = -\frac{1}{h_1 h_2} \frac{\partial h_2}{\partial x}, \quad K_2 = -\frac{1}{h_1 h_2} \frac{\partial h_1}{\partial z} \quad (4)$$

The boundary conditions for Eqs. (1–3) are

$$y = 0 \quad u, w = 0 \quad v = v_w(x, z) \quad (5a)$$

$$y = \delta \quad u = u_s(x, z) \quad w = 0 \quad (5b)$$

We note from Eq. (3) that if  $K_2$  is zero, a solution of Eq. (3) for the homogeneous boundary conditions is given by  $w = 0$ . It is evident from this that the action of the external stream curvature (for incompressible flow) is needed for the production of a cross flow. If  $K_2$  is small, then it can be expected that  $w$  is also small. This suggests a *small-cross flow* approximation in which terms of higher order in  $w$ ,  $K_2$  or lateral derivatives,  $(\partial/\partial z)$ , are neglected. In this case Eqs. (1–3) simplify considerably to the following equations known as the *boundary-layer equations for small cross flow*:

Continuity

$$(\partial/\partial x)(h_2 u) + (\partial/\partial y)(h_1 h_2 v) = 0 \quad (6)$$

Streamwise Momentum

$$\frac{u}{h_1} \frac{\partial u}{\partial x} + v \frac{\partial u}{\partial y} = \frac{u_s}{h_1} \frac{\partial u_s}{\partial x} + \frac{1}{\rho} \frac{\partial}{\partial y} \left( \mu \frac{\partial u}{\partial y} - \rho \overline{u'v'} \right) \quad (7)$$

Cross-Flow Momentum

$$\frac{u}{h_1} \frac{\partial w}{\partial x} + v \frac{\partial w}{\partial y} - K_1 u w = K_2 u_s^2 \left( 1 - \frac{u^2}{u_s^2} \right) + \frac{1}{\rho} \frac{\partial}{\partial y} \left( \mu \frac{\partial w}{\partial y} - \rho \overline{w'v'} \right) \quad (8)$$

Equations (1–3) form a highly nonlinear coupled system which is difficult to solve. In addition they contain the Reynolds shear-stress terms for which a closure assumption must be made. Obviously, for turbulent flows the accuracy of the solutions will depend on the closure assumptions. For this reason, in the study reported here we have somewhat simplified the mathematical problem by considering the boundary-layer equations for small

cross flow [Eqs. (6–8)] as well as the boundary-layer equations for *swept infinite cylinders*. The latter are given by the following equations:

Continuity

$$(\partial u/\partial x) + (\partial v/\partial y) = 0 \quad (9)$$

Chordwise Momentum

$$u \frac{\partial u}{\partial x} + v \frac{\partial u}{\partial y} = u_e \frac{du_e}{dx} + \frac{1}{\rho} \frac{\partial}{\partial y} \left( \mu \frac{\partial u}{\partial y} - \rho \overline{u'v'} \right) \quad (10)$$

Spanwise Momentum

$$u \frac{\partial w}{\partial x} + v \frac{\partial w}{\partial y} = \frac{1}{\rho} \frac{\partial}{\partial y} \left( \mu \frac{\partial w}{\partial y} - \rho \overline{w'v'} \right) \quad (11)$$

We have satisfied the closure assumptions through the eddy-viscosity concept and have related the Reynolds shear stresses to the mean velocity profiles. The next section describes our eddy-viscosity formulation.

### 3. Closure Assumptions for the Reynolds Shear Stresses

In order to satisfy the closure assumptions for the Reynolds shear stress terms, we use Boussinesq's eddy viscosity concept and define

$$-\rho \overline{u'v'} = \rho \varepsilon_1 (\partial u/\partial y), \quad -\rho \overline{w'v'} = \rho \varepsilon_2 (\partial w/\partial y) \quad (12)$$

For two-dimensional flows  $\varepsilon_1$  is defined by two separate formulas. According to the eddy-viscosity formulation used by Cebeci,<sup>3,4</sup> in the so-called inner region of the boundary layer  $\varepsilon_1$  is defined by a modified mixing-length expression and in the outer region  $\varepsilon_1$  is defined by an expression based on a velocity defect. For an incompressible flow,  $\varepsilon_1$  is given by the following formulas:

$$\varepsilon_1 = \begin{cases} L^2 \left| \frac{\partial u}{\partial y} \right| & 0 \leq y \leq y_c \\ \alpha \left| \int_0^\infty (u_e - u) dy \right| & y_c \leq y \leq \delta \end{cases} \quad (13)$$

where  $y_c$  is obtained from the continuity of eddy-viscosity. In the preceding equations  $L$  is a modified mixing-length expression given by

$$L = 0.4y \{1 - \exp(-y/A)\} \quad (14)$$

where

$$A = 26(v/N)u_e^{-1}, \quad u_e = (\tau_w/\rho)^{1/2} \quad (15a)$$

$$N = \left[ \frac{p^+}{v_w^+} \{1 - \exp(11.8v_w^+)\} + \exp(11.8v_w^+) \right]^{1/2}, \quad (15b)$$

$$p^+ = \frac{v u_e}{u_e^3} \frac{du_e}{dx}, \quad v_w^+ = \frac{v_w}{u_e}$$

The parameter  $\alpha$  in the outer eddy viscosity formula is generally assumed to be a universal constant equal to 0.0168. According to a recent study by Cebeci,<sup>6</sup> however, for values of  $R_\theta < 6000$ ,  $\alpha$  is not a universal constant; it varies with  $R_\theta$  as given by the following formula:

$$\alpha = \alpha_0(1 + \Pi_0)/(1 + \Pi) \quad (16a)$$

where  $\alpha_0 = 0.0168$ ,  $\Pi_0 = 0.55$ , and  $\Pi$ , which varies from 0 to 1.55 within a  $R_\theta$  range of 425–6000, is approximated by  $(\gamma \equiv R_\theta/425)^{-1}$

$$\Pi = 0.55[1 - \exp(-0.243\gamma^{1/2} - 0.298\gamma)] \quad (16b)$$

The eddy viscosity formulation (13) which is empirical like all methods for Reynolds stresses has worked well for two-dimensional flows and will be extended here for three-dimensional flows. In making this extension we will rely heavily on our experience with two-dimensional flows and carry over the empirical model used for the viscous layer<sup>4</sup> to three-dimensional flows.

To simplify the problem, we will first assume that  $\varepsilon_1 = \varepsilon_2$  and speculate on the  $\varepsilon_1$  formulation for small cross flows as well as swept infinite cylinders. Obviously, we should choose an eddy-viscosity formulation that should be invariant of the coordinate system used. For the inner region we will assume that

the inner eddy viscosity formula is given by the following expression:

$$\varepsilon_1 = L^2 [(\partial u / \partial y)^2 + (\partial w / \partial y)^2]^{1/2} \quad (17)$$

Here  $L$  is given by Eqs. (14) and (15) except that now the friction velocity  $u_\tau$  is given by

$$u_\tau = \left( \frac{\tau_s}{\rho} \right)^{1/2}, \quad \text{where} \quad \frac{\tau_s}{\rho} = \nu \left[ \left( \frac{\partial u}{\partial y} \right)_w^2 + \left( \frac{\partial w}{\partial y} \right)_w^2 \right]^{1/2} \quad (18a)$$

and the dimensionless pressure-gradient parameter  $p^+$  is given by

$$p^+ = (\nu u_s / u_\tau^3) (du_s / ds) \quad (18b)$$

In the outer region we will base our eddy viscosity expression on a resultant velocity defect defined by

$$u_s - (u^2 + w^2)^{1/2}$$

and write the outer eddy viscosity expression as

$$\varepsilon_o = \alpha \left| \int_0^\infty \{u_s - (u^2 + w^2)^{1/2}\} dy \right| \quad (19)$$

#### 4. Transformed Form of the Equations

The small cross-flow equations (6–8) as well as the swept-infinite-cylinder equations (9–11) are expressed in physical coordinates, and they are singular at  $x = 0$ . For this reason we first transform them to a coordinate system that removes the singularity and stretches the coordinate normal to the flow.

For the small cross-flow equations we define the stream function by

$$h_2 u = \partial \psi / \partial y, \quad h_2 v = -(1/h_1) (\partial \psi / \partial x) \quad (20)$$

and introduce the following transformation

$$ds = h_1 dx, \quad \eta = (u_s / \nu s)^{1/2} y \quad (21)$$

together with a dimensionless stream function  $f(s, \eta)$  defined by

$$\psi = (\nu u_s s)^{1/2} h_2 f \quad (22)$$

Using the relations (20–22) and the definition of eddy viscosity, we can write the streamwise and the cross-flow equations, (7) and (8), respectively, as follows:

Streamwise Momentum

$$(bf'')' + P[1 - (f')^2] + \left( \lambda_1 + \frac{P+1}{2} \right) f f'' = s \left( f' \frac{\partial f'}{\partial s} - f'' \frac{\partial f}{\partial s} \right) \quad (23)$$

Cross-Flow Momentum

$$(bg'')' - (\lambda_1 + P) f' g' + \left( \lambda_1 + \frac{P+1}{2} \right) f g'' + K_2 s [1 - (f')^2] = s \left( f' \frac{\partial g'}{\partial s} - g'' \frac{\partial f}{\partial s} \right) \quad (24)$$

where

$$f' = u/u_s, \quad g' = w/u_s, \quad \lambda_1 = s/h_2 \partial h_2 / \partial s, \\ P = s/u_s \partial u_s / \partial s, \quad h = 1 + \varepsilon^+$$

The boundary conditions are

$$\eta = 0; f = 0 \quad \text{or} \quad f = f_w \text{ (mass transfer), } f' = 0, \\ g = 0, \quad g' = 0 \quad (25a)$$

$$\eta = \eta_\infty; f' = 1, \quad g' = 0 \quad (25b)$$

For the swept infinite cylinder equations, we define the stream function by

$$u = \partial \psi / \partial y, \quad v = -\partial \psi / \partial x \quad (26)$$

introduce the Falkner transformation

$$x = x, \quad \eta = (u_s / \nu x)^{1/2} y \quad (27)$$

and the dimensionless stream function  $f(x, \eta)$  by

$$\psi = (u_s \nu x)^{1/2} f \quad (28)$$

Introducing Eqs. (26–28) into Eqs. (10) and (11), and using the definition of eddy viscosity we can write the transformed boundary-layer equations for swept infinite cylinders by the following equations:

Chordwise Momentum

$$(bf'')' + P[1 - (f')^2] + \frac{P+1}{2} f f'' = x \left( f' \frac{\partial f'}{\partial x} - f'' \frac{\partial f}{\partial x} \right) \quad (29)$$

Spanwise Momentum

$$(bg'')' + \frac{1}{2} f g'' = x \left( f' \frac{\partial g'}{\partial x} - g'' \frac{\partial f}{\partial x} \right) \quad (30)$$

where now

$$f' = u/u_e, \quad g' = w/w_e$$

The boundary conditions are

$$\eta = 0; f = 0, \quad \text{or} \quad f = f_w \text{ (mass transfer), } f' = 0, \\ g = 0, \quad g' = 0 \quad (31a)$$

$$\eta = \eta_\infty; f' = 1, \quad g' = 1 \quad (31b)$$

Similarly the eddy viscosity formulas (17) and (19) can be expressed in the transformed coordinates. For the small cross-flow transformation given by Eqs. (20–22), they become

$$\varepsilon_i^+ = 0.16 R_s^{1/2} \eta^2 \left[ 1 - \exp \left( -R_s^{-1/2} \eta \frac{s}{A} \right) \right]^2 [(f'')^2 + (g'')^2]^{1/2} \quad (32a)$$

$$\varepsilon_o^+ = 0.0168 R_s^{1/2} \left| \int_0^\infty [1 - \{(f')^2 + (g')^2\}^{1/2}] d\eta \right| \quad (32b)$$

where

$$R_s = u_s s / \nu$$

For the swept-cylinder transformation given by Eqs. (26–28), they become

$$\varepsilon_i^+ = 0.16 R_x^{1/2} \eta^2 \left[ 1 - \exp \left( -R_x^{-1/2} \eta \frac{x}{A} \right) \right]^2 \times \\ \left[ (f'')^2 + \left( \frac{w_e}{u_e} \right)^2 (g'')^2 \right]^{1/2} \quad (33a)$$

$$\varepsilon_o^+ = 0.0168 R_x^{1/2} \left| \int_0^\infty \left[ \frac{u_s}{u_e} - \left\{ (f')^2 + \left( \frac{w_e}{u_e} \right)^2 (g')^2 \right\}^{1/2} \right] d\eta \right| \quad (33b)$$

where

$$R_x \equiv u_e x / \nu \quad \text{and} \quad u_s = (u_e^2 + w_e^2)^{1/2}$$

#### 5. Numerical Method

We use a very efficient two-point finite-difference method to solve the system given by Eqs. (23–25) and the system given by Eqs. (29–31). This method was developed by H. B. Keller<sup>7</sup> and has successfully been applied to the two-dimensional boundary-layer equations by Keller and Cebeci. A detailed description of the method is presented in Refs. 1 and 2; for this reason only a brief description of it will be presented here.

In writing the difference equations, we shall only consider the system, Eqs. (23–25), namely, the small cross-flow equations. Later we will show that by setting certain terms equal to zero and by renaming some terms and by changing boundary conditions, we recover the system of Eqs. (29–31), namely, the swept infinite cylinder equations.

We first write the two momentum equations in terms of a first-order system of partial differential equations. For this purpose we introduce new dependent variables  $u(s, \eta)$ ,  $v(s, \eta)$ ,  $w(s, \eta)$  and  $t(s, \eta)$  so that Eqs. (23) and (24) can be written as

$$f' = u \quad (34a)$$

$$u' = v \quad (34b)$$

$$g' = w \quad (34c)$$

$$w' = t \quad (34d)$$

$$(bv)' + P(1 - u^2) + fv \left( \lambda_1 + \frac{P+1}{2} \right) = s \left( u \frac{\partial u}{\partial s} - v \frac{\partial f}{\partial s} \right) \quad (34e)$$

$$(bt)' + ft \left( \lambda_1 + \frac{P+1}{2} \right) - uw(\lambda_1 + P) + K_2 s(1 - u^2) = s \left( u \frac{\partial w}{\partial s} - t \frac{\partial f}{\partial s} \right) \quad (34f)$$

We next consider the net rectangle shown in Fig. 2. We denote the net points by

$$s_o = 0, \quad s_n = s_{n-1} + k_n, \quad n = 1, 2, \dots, N \quad (35)$$

$$\eta_o = 0, \quad \eta_j = \eta_{j-1} + h_j, \quad j = 1, 2, \dots, J; \quad \eta_J = \eta_\infty$$

The net spacings,  $k_n$  and  $h_j$ , are completely arbitrary and indeed may have large variations in practical calculations. This is especially important in turbulent boundary-layer calculations which are characterized by large boundary-layer thicknesses. To get accuracy near the wall, small net spacing is required while large spacing can be used away from the wall.

We approximate the quantities ( $f, u, v, q, w, t$ ) at points ( $s_n, \eta_j$ ) of the net by net functions denoted by ( $f_j^n, u_j^n, v_j^n, g_j^n, w_j^n, t_j^n$ ). We also employ the notation, for points and quantities midway between net points and for any net function  $q_j^n$

$$s_{n-1/2} \equiv \frac{1}{2}(s_n + s_{n-1}), \quad \eta_{j-1/2} \equiv \frac{1}{2}(\eta_j + \eta_{j-1}) \quad (36)$$

$$q_j^{n-1/2} \equiv \frac{1}{2}(q_j^n + q_j^{n-1}), \quad q_j^{n-1/2} \equiv \frac{1}{2}(q_j^n + q_j^{n-1})$$

The difference equations which are to approximate Eq. (34) are now easily formulated by considering one mesh rectangle as in Fig. 2. We approximate Eqs. (34a-d) using centered difference quotients and average about the midpoint ( $s_n, \eta_{j-1/2}$ ) of the segment  $P_2P_4$

$$(f_j^n - f_{j-1}^n)/h_j = u_{j-1/2}^n \quad (37a)$$

$$(u_j^n - u_{j-1}^n)/h_j = v_{j-1/2}^n \quad (37b)$$

$$(g_j^n - g_{j-1}^n)/h_j = w_{j-1/2}^n \quad (37c)$$

$$(w_j^n - w_{j-1}^n)/h_j = t_{j-1/2}^n \quad (37d)$$

Similarly Eqs. (34e-f) are approximated by centering about the midpoint  $s_{n-1/2}, \eta_{j-1/2}$  of the rectangle  $P_1P_2P_3P_4$ . This gives

$$\frac{(bv)_j^n - (bv)_{j-1}^n}{h_j} - (P_1^n + \alpha_n)(u^2)_{j-1/2}^n + (P_4^n + \alpha_n)(fv)_{j-1/2}^n + \alpha_n(f_{j-1/2}^n v_{j-1/2}^{n-1} - v_{j-1/2}^n f_{j-1/2}^{n-1}) = T_{j-1/2}^{n-1} \quad (37e)$$

(streamwise momentum)

$$\frac{(bt)_j^n - (bt)_{j-1}^n}{h_j} + (P_4^n + \alpha_n)(ft)_{j-1/2}^n - (P_6^n + \alpha_n)(uw)_{j-1/2}^n - P_5 s(u^2)_{j-1/2}^n - \alpha_n(u_{j-1/2}^{n-1} w_{j-1/2}^n - w_{j-1/2}^{n-1} u_{j-1/2}^n) - t_{j-1/2}^{n-1} f_{j-1/2}^n + f_{j-1/2}^{n-1} t_{j-1/2}^n = S_{j-1/2}^{n-1} \quad (37f)$$

(cross-flow momentum)

where

$$P_1 \equiv P, \quad P_2 \equiv (P+1)/2, \quad P_3 \equiv \lambda_1, \quad P_4 \equiv \lambda_1 + (P+1)/2 \quad (38a)$$

$$P_5 \equiv K_2, \quad P_6 \equiv \lambda_1 + P, \quad P_7 \equiv \lambda_1 + P_2$$

$$T_{j-1/2}^{n-1} = \alpha_n[(fv)_{j-1/2}^{n-1} - (u^2)_{j-1/2}^{n-1}] - P_1^n - \left[ \frac{(bv)_j^{n-1} - (bv)_{j-1}^{n-1}}{h_j} + P_1^{n-1} \{1 - (u^2)_{j-1/2}^{n-1}\} + P_4^{n-1}(fv)_{j-1/2}^{n-1} \right] \quad (38b)$$

$$S_{j-1/2}^{n-1} = \alpha_n[(ft)_{j-1/2}^{n-1} - (uw)_{j-1/2}^{n-1}] - P_5^n s^n - \left[ \frac{(bt)_j^{n-1} - (bt)_{j-1}^{n-1}}{h_j} + P_4^{n-1}(ft)_{j-1/2}^{n-1} - P_6^{n-1}(uw)_{j-1/2}^{n-1} + P_5^{n-1} s^{n-1} \{1 - (u^2)_{j-1/2}^{n-1}\} \right] \quad (38c)$$

$$\alpha_n \equiv s_{n-1/2}/(s_n - s_{n-1}) \quad (38d)$$

Equations (37) are imposed for  $j = 1, 2, \dots, j$  and the transformed boundary-layer thickness  $\eta_j$  is to be sufficiently large so that it is beyond the edge of the boundary layer. For most laminar flows  $\eta_j$  is constant. For turbulent flows, with no essential difficulty,  $\eta_j$  may be increased as the calculations

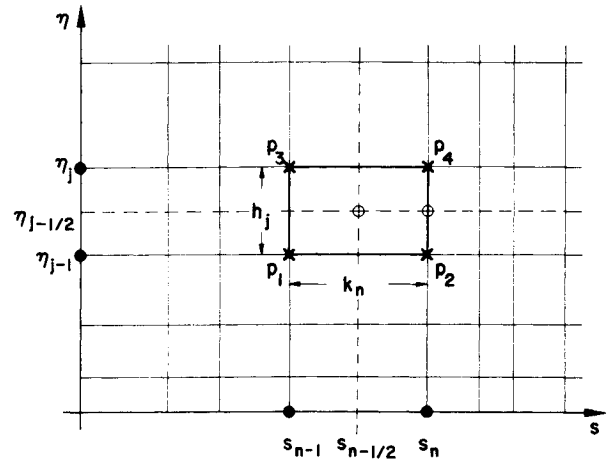


Fig. 2 Net rectangle for the difference equations.

proceed downstream from the point of transition. This is discussed in detail in Ref. 2.

The boundary conditions (25) yield at  $s = s_n$

$$f_o^n = f_w(s), \quad g_o^n = 0, \quad u_o^n = 0, \quad w_o^n = 0, \quad u_j^n = 1, \quad w_j^n = 0 \quad (40)$$

If we assume ( $f_j^{n-1}, u_j^{n-1}, v_j^{n-1}, g_j^{n-1}, w_j^{n-1}, t_j^{n-1}$ ) to be known for  $0 \leq j \leq J$  then Eq. (37) for  $1 \leq j \leq J$  and the boundary conditions (40) yield an implicit nonlinear algebraic system of  $6J+6$  equations in as many unknowns ( $f_j^n, j_j^n, v_j^n, g_j^n, w_j^n, t_j^n$ ). This system can be solved very effectively by using Newton's method. The details are presented in Ref. 2 so we do not repeat them here. The important observation is that the linearized equations obtained by applying Newton's method to Eqs. (37) and (40) form a block tridiagonal system (with  $6 \times 6$  blocks) and this system can be solved in a very efficient manner as discussed in Ref. 2.

The two differenced momentum equations given by (37e) and (37f) can be also used for swept infinite cylinders by setting  $s = x, u_s = u_e, \lambda_1 = 0, P_5 = 0, P_6 = 0$ , and  $P_7 = \frac{1}{2}$ . In addition the boundary conditions (40) are slightly different. They are given by  $f_o^n = f_w(s), g_o^n = 0, u_o^n = 0, w_o^n = 0, u_j^n = 1, w_j^n = 1$ .

## 6. Accuracy of the Method

The method discussed in the previous sections is applicable to both laminar and turbulent boundary layers. For laminar layers, the accuracy of the method depends on the accuracy of the numerical method. According to the study conducted in Ref. 1, the accuracy of the method is quite good for laminar flows. Highly accurate solutions can be obtained by taking 25 to 30 points across the boundary layer. Although a higher degree of accuracy can be obtained with less points by using Richardson extrapolation, the accuracy obtained with 25 to 30 points is sufficient for most laminar layers.

For turbulent flows, the accuracy of the method depends on the accuracy of the numerical method and on the accuracy of the model for the Reynolds stresses. Because the boundary-layer thickness is much larger in turbulent flows than in laminar flows, it is necessary to take more points across a turbulent layer. For laminar layers,  $\eta_\infty$ , namely, the transformed boundary-layer thickness, is nearly constant ( $=8$ ). For turbulent layers,  $\eta_\infty$  increases with Reynolds number. For example for a two-dimensional flat-plate flow  $\eta_\infty$  is approximately 100 at  $R_x = 10^8$ . In addition, because of the nature of a turbulent layer, it is necessary to use a variable grid across the layer to maintain the computational accuracy. Although a number of variable-grid systems can be used with the present method, here we use the net used earlier by Cebeci and Smith<sup>3</sup> in two-dimensional flows. It is given by

$$\eta_j = h_1(K^j - 1)/(K - 1) \quad j = 1, 2, 3, \dots, J \quad (41)$$

In Eq. (41) there are two parameters:  $h_1$ , the length of the first  $\Delta\eta$ -step, and  $K$ , the ratio of two successive steps,  $K \equiv h_j/h_{j-1}$ . The total number of points across the layer can be calculated by the following formula:

$$J = \frac{\ln [1 + (K-1)\eta_\infty/h_1]}{\ln K} \quad (42)$$

In our calculations we select the parameters  $h_1$  and  $K$  and calculate the  $\eta_\infty$ . Several runs with a different number of points across the boundary layer showed that approximately 40 to 50 points are sufficient for turbulent flows. A typical value of  $h_1$  is 0.01, provided that the Reynolds number is not very large, say less than  $10^7$ . At higher Reynolds numbers, it is better to use a smaller value of  $h_1$ , say  $h_1 = 0.005$ . Figure 3 shows the values of  $K$  for various values of  $(\eta_\infty/h_1) \times 10^{-2}$  and  $J$ . From this figure we choose the value of  $K$  as follows:

Let us assume that we want to take a maximum of 50 points across the boundary layer. If the Reynolds number is not very large, an estimate for the maximum value of  $\eta_\infty = 100$  is sufficient. Then, taking  $h_1 = 0.01$ , the ratio  $(\eta_\infty/h_1) \times 10^{-2}$  is 100. Thus from Fig. 3,  $J = 50$ ,  $K$  is approximately 1.16.

Once the accuracy of the numerical method is established, it is next necessary to establish the accuracy of the model for the Reynolds shear stress. This is done in the next section.

## 7. Comparison With Experiment and With Bradshaw's Method

There are several experimental data for incompressible turbulent boundary-layer flows past infinite swept wings. In Ref. 5 Bradshaw gives a good description of these flows and also presents results obtained by his method. In this section we consider the same flows and compare our predictions with experiment and with those given by Bradshaw. It should be noted, however, that in making these comparisons it is necessary to specify the initial velocity profiles to start the calculations. Reference 14 describes our procedure for the initial profiles. Unless otherwise specified, all calculations reported here were made by solving the swept-infinite cylinder equations.

The definitions of some of the terms used in making the comparisons presented in the next section are as follows. To calculate the cross-flow angle  $\beta$ , it is necessary to know the cross-flow velocity and the streamwise velocity as well as the cross-flow wall shear and the streamwise wall shear. To distinguish the various velocity definitions in this section and in the following sections, for convenience, we shall use  $u_n$  and  $u_s$  to

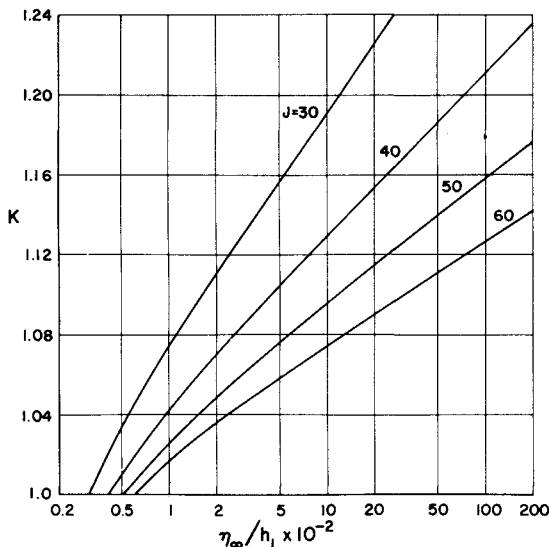


Fig. 3 Variable-grid parameter for given step size and boundary-layer thickness.

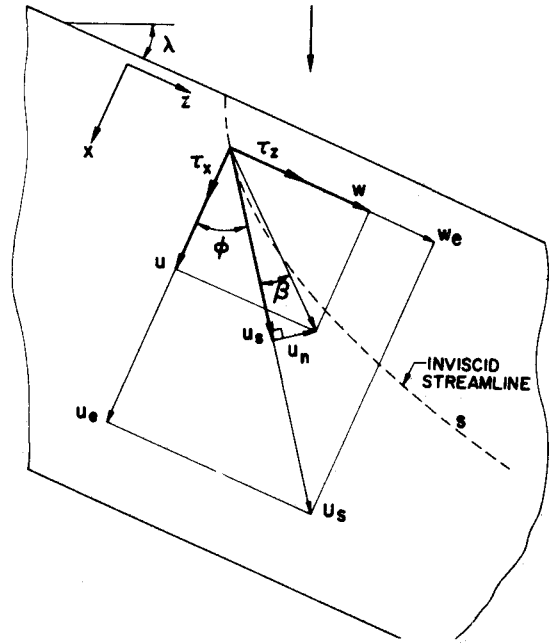


Fig. 4 Sketch showing the definitions of various coordinates and velocities.

represent the cross-flow and streamwise velocities, respectively. The streamwise velocity at the edge shall be represented by  $U_s$ . Similarly  $\tau_n$  and  $\tau_s$  shall represent the cross-flow and streamwise shear stresses, respectively. For nomenclature see Fig. 4.

The wall cross-flow angle  $\beta_w = \tan^{-1} (\tau_n/\tau_s)_w$  can be obtained as follows:

$$\tau_n = \tau_x \cos \phi - \tau_y \sin \phi \quad (43a)$$

$$\tau_s = \tau_x \cos \phi + \tau_y \sin \phi \quad (43b)$$

where

$$\phi = \tan^{-1} (w_e/u_e) \quad (44)$$

Using the transformation (26–28) and the relations (43), we can write the wall cross-flow angle as

$$\beta_w = \tan^{-1} \frac{g_w'' \cos \phi - f_w'' \sin \phi}{f_w'' \cos \phi + g_w'' \sin \phi} \quad (45)$$

From Fig. 4, we can write

$$u_n = w \cos \phi - u \sin \phi \quad (46a)$$

$$u_s = u \cos \phi + w \sin \phi \quad (46b)$$

Since

$$u_e = U_s \cos \phi, \quad w_e = U_s \sin \phi$$

we can write Eqs. (46) as

$$\frac{u_n}{U_s} = \left( \frac{w}{w_e} - \frac{u}{u_e} \right) \sin \phi \cos \phi \quad (47a)$$

$$\frac{u_s}{U_s} = \frac{u}{u_e} \cos^2 \phi + \frac{w}{w_e} \sin^2 \phi \quad (47b)$$

From the definitions of cross-flow angle and  $f'$  and  $g'$  it follows that

$$\beta = \tan^{-1} \frac{(g' - f') \sin \phi \cos \phi}{f' \cos^2 \phi + g' \sin^2 \phi} \quad (48)$$

The local streamwise skin-friction coefficient,  $c_{f_s}$ , is defined as follows:

$$c_{f_s} = \tau_{w_s} / \frac{1}{2} \rho U_s^2 \quad (49)$$

In terms of  $c_{f_x}$

$$c_{f_x} = \tau_{w_x} / \frac{1}{2} \rho u_e^2 = 2f_w'' / (R_x)^{1/2} \quad (50a)$$

and  $c_{f_z}$

$$c_{f_z} = \tau_{w_z} / \frac{1}{2} \rho w_e^2 = 2(w_e/u_e)^2 g_w'' / (R_x)^{1/2} \quad (50b)$$

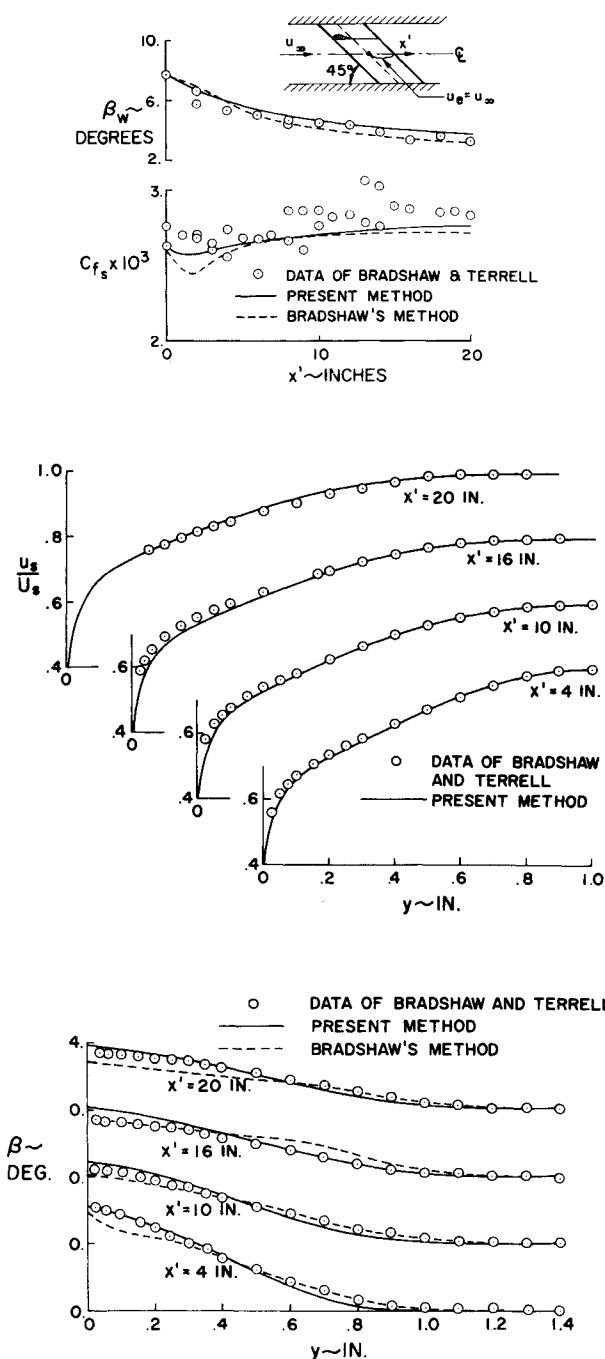


Fig. 5 Results for the relaxing flow of Bradshaw and Terrell: a) wall cross flow angle and local skin friction; b) velocity profiles; c) cross flow angle distributions.

we can write Eq. (49) as follows:

$$c_{fs} = c_{fx} \cos^3 \phi + c_{fz} \sin^3 \phi \quad (51)$$

#### 7.1 45° "Infinite" Swept Wing, Data of Bradshaw and Terrell

This experiment<sup>8</sup> was set up especially to test the outer-layer assumptions made in extending the boundary-layer calculation method of Bradshaw et al.<sup>9</sup> from two dimensions to three. Measurements were made only on the flat rear of the wing in a region of nominally zero pressure gradient and decaying cross flow. See the sketch in Fig. 5a. Spanwise and chordwise components of mean velocity and shear stress, and all three components of turbulence intensity, were measured at a number of distances  $x' = 0, 4, 10, 16$ , and 20 in. from the start of the flat portion of the wing (see Fig. 5). The surface shear stress,

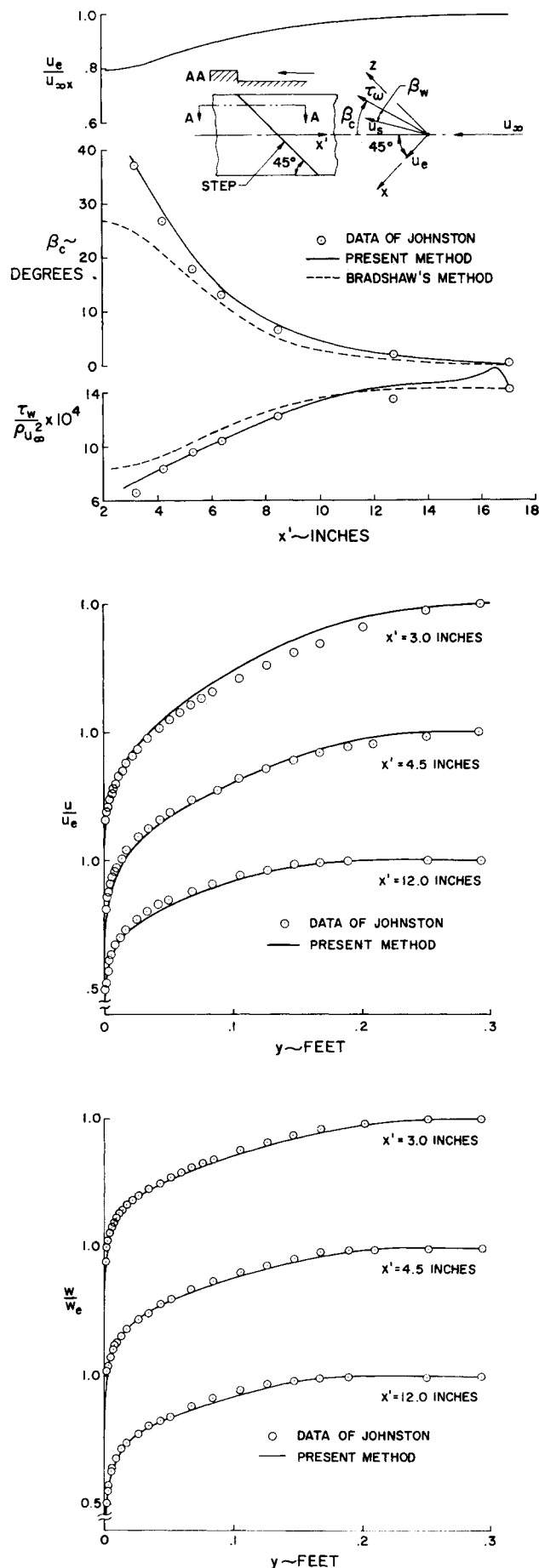


Fig. 6 Results for infinite swept forward-facing step: a) wall cross flow angle and shear; b) chordwise velocity profiles; c) spanwise velocity profiles.

measured with a Preston tube, was constant along a generator at the start of the flat part of the wing, except for a few inches at each end and except for small undulations of small spanwise wave length caused by residual nonuniformities in the tunnel flow.

Figure 5 shows the calculated results compared with experimental results and those obtained by Bradshaw's method.<sup>5</sup> Our calculations were started at  $x' = 0$  by using the procedure described in Ref. 14. The initial values for  $c_{fs}$  and  $R_{\delta_1^*}$  were taken as  $2.62 \times 10^{-3}$  and  $1.13 \times 10^4$ , respectively. Also, the cross-flow angle distribution, given by experiment, was used in the initial velocity profile.

7.2 45° "Infinite" Swept Forward-Facing Step, Data of Johnston<sup>10</sup>

This experiment<sup>10</sup> was set up to check the limits of accuracy of the mixing length distribution near the surface. The boundary layers were measured upstream of a 45° "infinite" swept forward-facing step. The step height was 2 in., the boundary-layer thickness at  $x = -17$  in., near the start of the pressure gradient, being 2.1 in. See the sketch in Fig. 6a. The flow in the outer part of this strongly retarded boundary layer depends far more on the pressure gradient than on the shear-stress gradient.

Figure 6 shows the results for this case. Our calculations were started at  $x = -17$  in. The initial values for  $c_{fs}$  and  $R_{\delta_1^*}$  were taken as  $2.86 \times 10^{-3}$  and  $1.21 \times 10^4$ , respectively. The initial cross-flow angle distribution was zero.

The computed centerline cross-flow angle  $\beta_c$ , defined by,  $\beta_c = \beta_w + \phi - 45$  and dimensionless wall shear-stress,  $\tau_w/\rho u_\infty^2$ , shown in Fig. 6a, are in very good agreement with experiment. It is seen from Fig. 6a that Bradshaw's computed values begin to deviate significantly from the experimental data as the flow approaches the step.

Figures 6b and 6c show a comparison of calculated and experimental velocity profiles in the  $x$ - and  $z$ -directions. As seen, away from the step the agreement with experiment is excellent. As the flow approaches the step, the velocity profiles begin to deviate slightly from experiment.

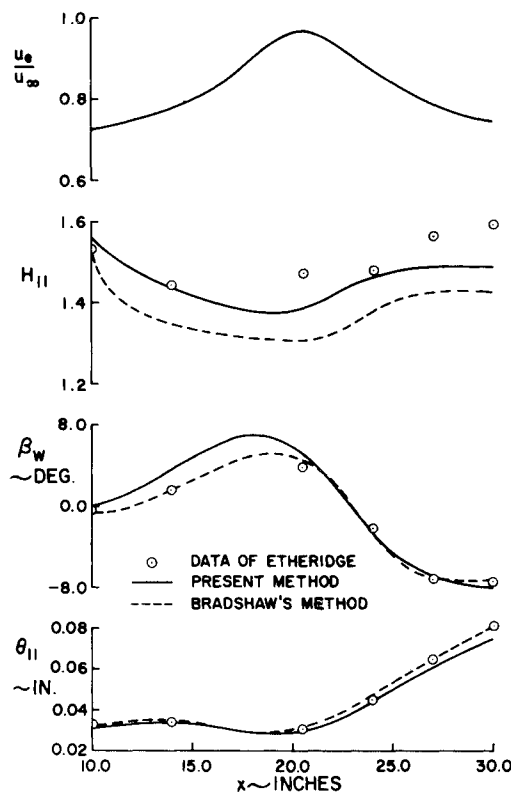


Fig. 7 Calculated results for the data of Etheridge.

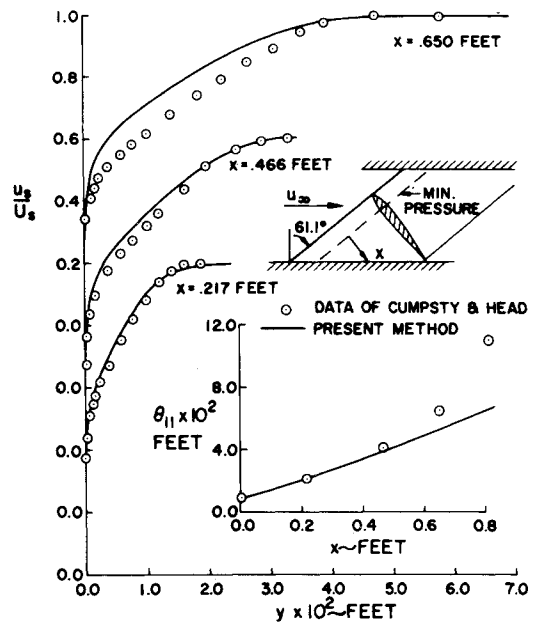


Fig. 8 Calculated results for the data of Cumpsty and Head on the rear of a swept infinite wing.

7.3 45° "Infinite" Swept Plate With Externally-Imposed Pressure Gradient, Data of Etheridge<sup>11</sup>

In this experiment<sup>11</sup> the pressure gradient, imposed by a swept cylinder above the plate, was at first strongly favorable and then moderately adverse. According to Bradshaw<sup>5</sup> values of  $p^+$  approached 0.01 so that laminarization may have been imminent.

Figure 7 shows the results for the experimental data of Etheridge. In this case we did not have access to the experimental data so we used the pressure distribution given in Bradshaw's paper, together with the same initial conditions used by Bradshaw.<sup>12</sup> According to the comparisons presented in Fig. 7, the shape factor values calculated by the present method are in better agreement than those calculated by Bradshaw's method. On the other hand, cross-flow angle and momentum thickness values calculated by Bradshaw's method are in better agreement than the present calculated values.

7.4 61.1° "Infinite" Swept Wing, Data of Cumpsty and Head<sup>12</sup>

In this experiment the boundary-layer development was measured on the rear of a wing swept at 61.1°. The boundary layer separated at about 80% chord. The measured profiles were affected by traverse gear "blockage," probably because of upstream influence of disturbance caused to the separated flow by the wake of the traverse gear.

Figure 8 shows the results. The calculations were made by using the measured pressure distribution given by "downstream tappings" as presented in Fig. 3 of Ref. 13. They were started at  $x = 0$  ( $x$  in this case denotes the distance measured from the minimum pressure point) with the following initial values

$$c_{fs} = 4.1 \times 10^{-3}, \quad R_{\delta_1^*} = 1.660 \times 10^3$$

The experimental cross-flow profile at  $x = 0$  was slightly S-shaped; for this reason, we have assumed  $\beta = 0$ , at this station.

The calculated velocity profiles in Fig. 8 show good agreement with experiment at two  $x$ -stations. However, with increasing distance they begin to deviate from experimental values and at  $x = 0.650$  ft, the agreement becomes poor.

For this experiment we have not compared our calculated results with Bradshaw's results since his calculations were made for a sweep angle of 62.5°. However, Bradshaw's results should not be much different than those calculated by the present method.

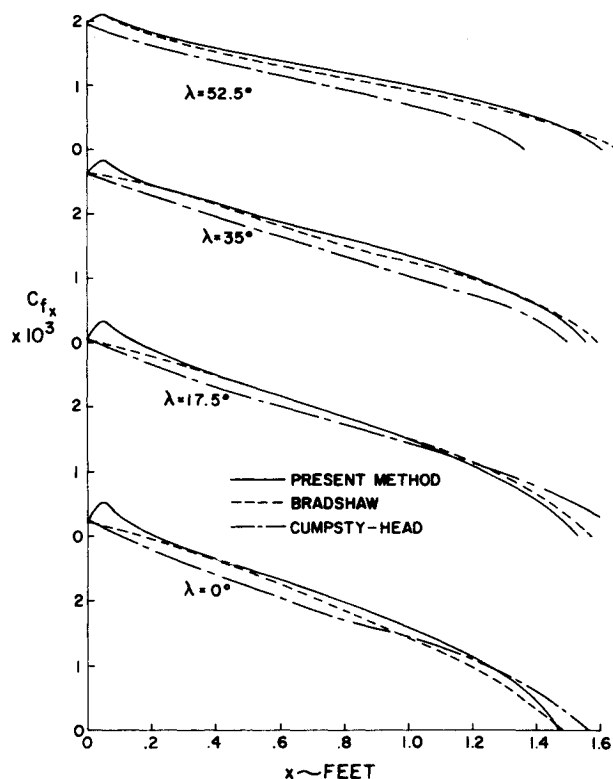


Fig. 9 Calculated results for the "Dummy" test cases of Cumpsty and Head: a) local skin friction.

### 7.5 "Dummy" Test Cases of Cumpsty and Head<sup>14</sup>

In Ref. 14 Cumpsty and Head made calculations for several "dummy" test cases by using their entrainment method. They assumed a constant linear gradient of chordwise velocity and varied the sweep angle. In Ref. 5, Bradshaw made the same calculations by using his method and showed that the predictions of his method disagreed fairly strongly with Cumpsty and Head's entrainment method.

Here we have made the same calculations and compared our predictions with those given by Bradshaw<sup>5</sup> and Cumpsty and Head.<sup>14</sup> Calculations were made for sweep angles of  $0^\circ$ ,  $17.5^\circ$ ,  $35^\circ$ , and  $52.5^\circ$  for the external velocity distribution given by

$$u_e = \begin{cases} U_\infty \cos \lambda, & x < 0 \\ U_\infty \cos \lambda(1 - 0.25x), & x > 0 \end{cases}$$

where  $x$  is measured from the start of the adverse pressure gradient. For all calculations the initial values of  $c_{f_s}$  and  $R_{\delta_1^*}$  were taken as

$$c_{f_s} = 3.22 \times 10^{-3}, \quad R_{\delta_1^*} = 3.79 \times 10^3$$

Fig. 9 shows that the calculated values agree well with those calculated by Bradshaw's method and disagree fairly strongly with those calculated by the entrainment method of Cumpsty and Head.

### References

- Keller, H. B. and Cebeci, T., "Accurate Numerical Methods for Boundary Layers. I. Two-Dimensional Laminar Flows," *Proceedings of the Second International Conference on Numerical Methods in Fluid Dynamics, Lecture Notes in Physics*, Vol. 8, Springer-Verlag, New York, 1971.
- Keller, H. B. and Cebeci, T., "Accurate Numerical Methods for Boundary Layers. II. Two-Dimensional Turbulent Flows," *AIAA Journal*, Vol. 10, No. 9, Sept. 1972, pp. 1197-1200.
- Cebeci, T. and Smith, A. M. O., "A Finite-Difference Method for Calculating Compressible Laminar and Turbulent Boundary Layers," *Journal of Basic Engineering*, Vol. 92, No. 3, Sept. 1970, pp. 523-535.
- Cebeci, T., "The Behavior of Turbulent Flow Near a Porous Wall with Pressure Gradient," *AIAA Journal*, Vol. 8, No. 12, Dec. 1970, pp. 2152-2156.
- Bradshaw, P., "Calculation of Three-Dimensional Turbulent Boundary Layers," *Journal of Fluid Mechanics*, Vol. 46, Pt. 3, 1971, pp. 417-445.
- Cebeci, T., "Kinematic Eddy Viscosity at Low Reynolds Numbers," *AIAA Journal*, Vol. 11, No. 1, Jan. 1973, p. 102.
- Keller, H. B., "A New Difference Scheme for Parabolic Problems," *Numerical Solution of a Partial Differential Equations*, Vol. II., edited by J. Bramble, Academic Press, New York, 1970.
- Bradshaw, P. and Terrell, M. G., "The Response of a Turbulent Boundary Layer on an Infinite Swept Wing to the Sudden Removal of Pressure Gradient," *Aero Rept. 1305*, 1969, National Physical Lab., London, England.
- Bradshaw, P., Ferriss, D. H., and Atwell, N. P., "Calculation of Boundary Layer Development Using the Turbulent Energy Equation," *Journal of Fluid Mechanics*, Vol. 28, Pt. 3, 1967, pp. 593-616.
- Johnston, J. P., "Measurements in a Three-Dimensional Turbulent Boundary Layer Induced by a Swept, Forward Facing Step," *Journal of Fluid Mechanics*, Vol. 42, Pt. 4, 1970, pp. 823-844.
- Etheridge, D., Ph.D. thesis, 1970, Queen Mary College, London University, London, England.
- Bradshaw, P., private communication, Imperial College of Science and Technology, London, England.
- Cumpsty, N. A. and Head, M. R., "The Calculation of Three-Dimensional Turbulent Boundary Layers. Part IV: Comparison of Measurements with Calculations on the Rear of a Swept Wing," *C.P. 1077*, 1970, Aeronautical Research Council, London, England.
- Cumpsty, N. A. and Head, M. R., "The Calculation of Three-Dimensional Turbulent Boundary Layers. Part I: Flow over the Rear of an Infinite Swept Wing," *Aeronautical Quarterly*, Vol. 18, 1967, pp. 55-84.
- Cebeci, T., Mosinskis, G. J., and Kaups, K., "A General Method for Calculating Three-Dimensional Incompressible Laminar and Turbulent Boundary Layers. I. Swept Infinite Cylinders and Small Cross Flow," *Rept. MDC J5694*, 1972, Douglas Aircraft Co., Long Beach, Calif.